Theory of C_2H_x Species on Pt{110}(1 × 2): Structure, Stability, and Thermal Chemistry

Alexandra T. Anghel,* Stephen J. Jenkins, David J. Wales, and David A. King*

Department of Chemistry, University of Cambridge, Lensfield Road, Cambridge CB2 1EW, U.K.

Received: September 11, 2005; In Final Form: December 13, 2005

The adsorption of C_2H_x ($x = 0-5$) hydrocarbon fragments on Pt{110}(1 × 2) has been investigated using calculations based on density functional theory. For all the species, the most stable adsorption site identified completes the tetravalency of each carbon atom and involves the maximum possible number of Pt atoms subject to that constraint. The most stable adsorption sites for C_2H_x fragments of stoichiometry $x = 2-5$ involve ridge atoms, while trough sites stabilize C_2H and C_2 species. The relative stability of the fragments involved is compared via a free energy picture.

Introduction

A large number of industrially relevant processes such as catalytic steam cracking of ethane,[1] alkene hydrogenation,[2,3] Fischer−Tropsch synthesis,[4,5] and catalytic hydrocarbon oxidation are crucially influenced by the stability and reactivity of C_2H_x hydrocarbon fragments at metal surfaces. These processes are selectively catalyzed by a small group of transition metals and alloys, including platinum and bimetallic alloys such as platinum−gold, platinum−iridium, and platinum−rhenium. Adsorption is often accompanied by the evolution of hydrogen, with C−H bonds being much more easily activated than C−C bonds.[6−8] The stability and hydrogenation of unsaturated C_2H_x hydrocarbons has been extensively studied using a large number of experimental surface science techniques on a variety of transition metal surfaces. In particular, the stability of C_2H_3 species adsorbed at metal surfaces has been the subject of great debate and is of significant industrial importance.[6] For example, the selective catalytic conversion of ethene to functionalized olefins, such as vinyl chloride, vinyl acetate, and vinyl alcohols, over supported metal catalysts may involve the formation of a surface vinyl intermediate ($HC-CH_2$).[2] This species could then react with a nucleophilic reagent such as acetic acid, chlorine, or water to give the functionalized olefin.

In contrast, recent supersonic molecular beam studies revealed that the stable dissociation product of C_2H_6 on Pt{110}-(1 × 2) has C_2H_2 stoichiometry at all coverages in the surface temperature range 350−400 K.[9] Temperature-programmed reaction (TPR) experiments further showed that C_2H_2 decomposes to C−CH above 400 K, with a reaction-limited peak temperature of 430 K.[9] Stuck et al.[10] found that the calorimetric differential heat on adsorbing ethene (H_2C-CH_2) on Pt{110} drops in several steps with increasing coverage at 300 K. They ascribed these steps to formation of both C_2H_2 and C_2H_3 on the surface, based on combined electron energy loss spectroscopy (HREELS) and comparison with thermal desorption results by Yagasaki et al.[11]

Below 200 K, ethene adsorption on Pt{111} is molecular.[12] Both di-σ and π-bonded ethene have been identified using second-harmonic generation[13] and infrared spectroscopy.[14−16] The di-σ species was initially formed upon ethene adsorption, while the π species was characterized as the system became pressurized. Land et al.,[17] using variable temperature scanning tunneling microscopy, have imaged a long-range ethene superstructure on Pt{111} at 160 K, which upon annealing to 350 K gave ethylidyne ($C-CH_3$) as the only stable surface species. Interestingly, the vinyl radical ($HC-CH_2$), which is the direct product of a straightforward C−H bond activation in ethene, has not as yet been detected over close-packed {111} metal surfaces. Zaera et al.[18] found that ethene hydrogenates via a stepwise incorporation of hydrogen atoms on Pt{111}. Under high H_2 pressures, however, a strongly bonded $C-CH_3$ species was found to form preferentially at a threefold hollow site.[18]

We note in passing that ethene chemistry on Pd{111} is similar to that on Pt{111}.[19] A density functional theory (DFT) study has found that π and di-σ ethene forms have similar stability in a (2 × 2) unit cell on Pd{111},[20] while a combined reflection adsorption infrared spectroscopy (RAIRS) and molecular beam study has detected a substantial rehybridization upon adsorbing ethene on the clean surface at low surface temperatures.[21] In the analysis that follows, we will frequently refer back to results obtained on Pd{111}[22] as a reasonable model for the Pt{111} surface. Where such data are available, a comparison to slab DFT results for C_2H_x adsorption on Pt{111}[23−25] is also given.

Much progress has been made in understanding the interaction of C_2H_x fragments with metal surfaces using experimental techniques.[6] However, there still remains much to be done. Furthermore, the large number of possible bonding geometries has, hitherto, made comprehensive theoretical studies of C_2H_x dehydrogenation pathways and products unfeasible. It has only recently become possible to study these systems using theoretical tools, thanks to continued increases in available computer power and improved geometry optimization techniques. In this article, we report DFT results for the stability and structure of C_2H_x ($x = 0-5$) hydrocarbon fragments on the missing-row reconstructed Pt{110}(1 × 2) surface. This work is a natural progression from a previous DFT study, which investigated CH_3 stepwise dehydrogenation to give adsorbed C atoms on Pt{110}-(1 × 2).[26,27]

Computational Details

Calculations were performed using DFT and the CASTEP code.[28] The parameters and computational model employed were the same as those described in detail in other recent papers.[29,30] The top three surface layers and the hydrocarbon species were

* E-mail: ata22@cam.ac.uk (A.T.A.); dak10@cam.ac.uk (D.A.K.).

10.1021/jp055128n CCC: $33.50
Published on Web 02/11/2006

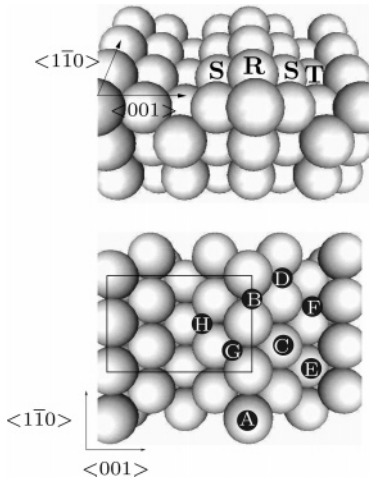

Figure 1. The missing-row reconstructed Pt{110}(1 × 2) surface. R, S, and T denote ridge, second-layer, and trough surface sites. C_2H_x adsorption was investigated at the sites labeled. The highlighted rectangle indicates the (2 × 2) unit cell employed.

allowed to relax during geometry optimization. C_2H_x ($x = 0-5$) adsorption was studied on Pt{110}(1 × 2) at all surface sites, as depicted in Figure 1. The adsorbate coverage of 0.25 monolayers (ML) was obtained by placing one C_2H_x hydrocarbon fragment in the depicted (2 × 2) unit cell on the missing-row reconstructed side of the Pt{110} slab. This coverage corresponds to that found experimentally for C_2H_x products during ethane dissociative adsorption.[9] At higher coverages, we expect repulsive interactions between the adsorbed hydrocarbon species to become significant, but at the low coverage studied, lateral interactions are considered negligible. Multiple C_2H_x orientations were investigated at each surface site, to maximize the chances of identifying the most stable structures.

Throughout this work, C_2H_x chemisorption energies are reported with respect to the same reference reactant state. This common state was taken to be gaseous C_2H_6 and a (2 × 2) cell of the clean Pt{110} surface, denoted by $C_2H_6^{gas}$ and $Pt_{110}^{(2\times2)}$ in the following reaction scheme:[25]

$$C_2H_6^{gas} \rightarrow C_2H_x^{gas} + \frac{1}{2}(6-x)H_2^{gas} \quad (1)$$

$$Pt_{110}^{(2\times2)} + C_2H_x^{gas} \rightarrow C_2H_x^{ads} \quad (2)$$

$$(6-x)Pt_{110}^{(2\times2)} + \frac{1}{2}(6-x)H_2^{gas} \rightarrow (6-x)H^{ads} \quad (3)$$

Summing the above equations gives

$$(7-x)Pt_{110}^{(2\times2)} + C_2H_6^{gas} \rightarrow C_2H_x^{ads} + (6-x)H^{ads} \quad (4)$$

where surface chemisorbed species are denoted by the superscript "ads" and the gaseous species by the superscript "gas". The site for hydrogen adsorption in the (2 × 2) unit cell is taken to be over a ridge bridge site, previously found to be the most stable site by Petersen et al.[26,27] In this adsorption model, the $C_2H_x^{ads}$ and $(6-x)H^{ads}$ products of ethane dehydrogenation on $Pt_{110}^{(2\times2)}$ are treated as if they are adsorbed on separate Pt{110} slabs, thus mimicking perfect phase separation on the real surface.

Results

The relative stability of C_2H_x metastable species is reported below. Only the three structures lowest in energy for each stoichiomtery are shown; the remainder of the structures in the Supporting Information. For simplicity, only the repeating unit cell is shown in the following figures, where the atomic colors are as follows: gray for platinum, green for carbon, and black for hydrogen.

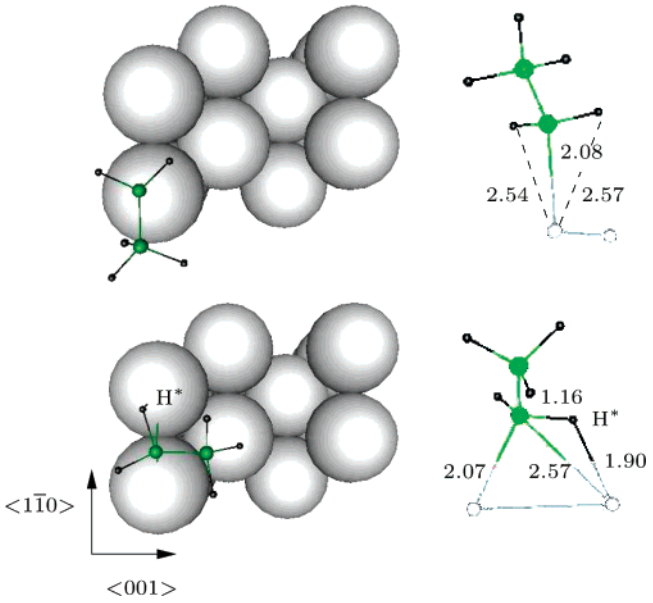

Figure 2. The most stable C_2H_5 structure found on Pt{110} is depicted at the top; a metastable intermediate structure is shown at the bottom. The right-hand image in each case is rotated to provide the clearest view of the molecular geometry. Bond lengths are given in angstroms. H* denotes the H atom interacting with the surface.

Adsorbed C_2H_5. During geometry optimization, the hydrocarbon fragment was found to drift from the second layer and trough surface sites toward the ridge or the gas phase. For all converged structures above the ridge, the C−C axis was found to tilt upward somewhat with respect to the surface plane. The most stable chemisorbed system found, shown in the top panel of Figure 2, involves ethyl (C_2H_5) bonding to the surface at a ridge atop site through a single C atom. C_2H_5 adsorbed at a ridge atop site in a staggered-like conformation is found to be 0.10 eV more stable than the corresponding eclipsed form. For the staggered conformers, alignment of the C−C axis along the $\langle 1\bar{1}0\rangle$ or $\langle 001\rangle$ direction gives isoenergetic structures, with an enthalpy change for dissociative adsorption (using the reaction scheme in eq 4) exothermic by −0.44 eV. In the depicted structure, the C−C bond length is 1.50 Å, with the shortest C−Pt bond equaling 2.09 Å and all C−H bond lengths at 1.09 Å. This structure is in good agreement with those found in previous slab DFT studies of C_2H_5 adsorption on Pt{111}[25] and Pd{111}[22] in (2 × 2) unit cells, which also found that adsorption is energetically preferred at atop surface sites, with C−C bond lengths of 1.51 Å for both Pt{111} and Pd{111}. The shortest C−metal distances were found to be 2.14 Å on Pt{111}[25] and 2.08 Å on Pd{111}.[22] On the basis of enthalpy considerations alone, the current theoretical study finds that partial dissociation of gas-phase ethane on Pt{110}(1 × 2) is an exothermic process, in contrast to the Pt{111} case, where dissociation is endothermic by 0.18 eV.[25]

A metastable system, shown in the bottom panel of Figure 2, where C_2H_5 is adsorbed at a ridge bridge site, was also characterized in the present study. This structure is 0.18 eV less stable than the apparent global minimum described above. The carbon atom bonds more closely to one of the ridge surface atoms that it bridges, with the corresponding C−Pt distances being 2.08 Å and 2.57 Å, respectively. For this configuration,

TABLE 1: Relative Stability of C_2H_x ($x = 4$ to 0) on Pt{110}[a]

stoichiometry	H_2C-CH_2	E_{rel}	$HC-CH_3$	E_{rel}
C_2H_4	1	0.00	1	0.23
	2	0.14	2	0.69
	3	0.28	3	0.71
stoichiometry	$C-CH_3$	E_{rel}	$HC-CH_2$	E_{rel}
C_2H_3	1	0.00	1	0.13
	2	0.06	2	0.31
	3	0.33	3	0.36
stoichiometry	HC−CH	E_{rel}	$C-CH_2$	E_{rel}
C_2H_3	1	0.00	1	0.03
	2	0.28	2	0.28
	3	0.29	3	0.30
stoichiometry	C−CH	E_{rel}		
C_2H	1	0.00		
	2	0.49		
	3	0.52		
stoichiometry	C−C	E_{rel}		
C_2	1	0.00		
	2	0.44		
	3	1.26		

[a] The energies, E_{rel}, are in eV. The chemisorbed minimum for each C_2H_x stoichiometry was chosen as the arbitrary zero of energy for that stoichiometry. Structures are labeled according to Figures 3−10.

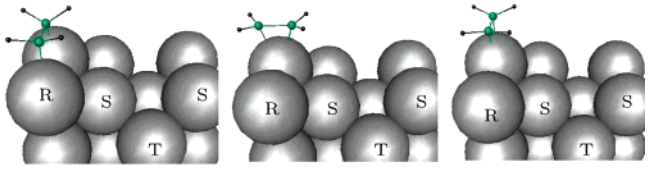

Figure 3. Ethene chemisorbed local minima on Pt{110} numbered according to their relative energetic stabilities: 1 indicating the most stable, and 3 the least.

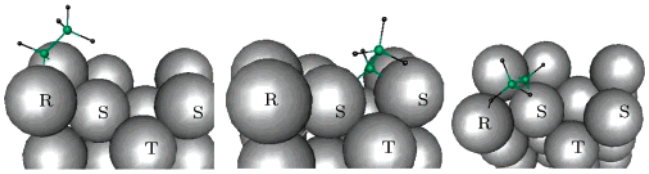

Figure 4. Ethylidene chemisorbed local minima on Pt{110} numbered according to relative energetic stability: 1 being the most stable, and 3 the least.

one carbon−hydrogen bond, labeled C−H* in Figure 2, interacts with the Pt surface, leading to a weakening and hence lengthening of this bond to 1.16 Å. The H*−Pt bond involved has shortened to 1.90 Å. The C−C bond is unaffected, with a length of 1.50 Å. Previously, agostic-type interactions have been reported for C_2H_5 adsorption at fcc/hcp sites on Pt{111}[25] and for CH_3 at a ridge bridge site on Pt{110}(1 × 2).[26] However, this structure is not found to be a reaction intermediate for pathways involving dehydrogenation of chemisorbed C_2H_5 on Pt{110}(1 × 2), which we reported previously.[30]

Adsorbed H_2C-CH_2 and $HC-CH_3$. Nine distinct ethene (H_2C-CH_2) and ten distinct ethylidene ($HC-CH_3$) structures were characterized. The relative energies and geometries for the three structures lowest in energy are given in Table 1 and Figures 3 and 4.

Ethene is found to be the most stable C_2H_4 species adsorbed on the surface. In this structure, labeled 1 in Figure 3, the hydrocarbon bonds in a di-σ like fashion to neighboring ridge Pt sites. The C−C bond is 1.46 Å long and is aligned along the $\langle 1\bar{1}0 \rangle$ surface direction. Each carbon atom is positioned equidistant from neighboring ridge surface atoms, with the shortest C−Pt distance being 2.08 Å. The four symmetry-equivalent C−H bonds are orientated at 115.5° to the C−C axis, suggesting that the degree of saturation in the adsorbed hydrocarbon fragment has increased in comparison to gaseous ethene, where the corresponding angle would have been 122.2°.[31] A di-σ H_2C-CH_2 geometry, for which the molecular plane is also tilted, has been previously experimentally observed on Pt{111} using high-resolution electron energy loss spectroscopy (HREELS),[32] UPS,[33] and NEXAFS.[34] For our structure, the enthalpy for dissociative adsorption with respect to gaseous ethane and the clean surface (using eq 4) is exothermic by −1.07 eV, while the adsorption enthalpy with respect to gaseous ethene is exothermic by −1.57 eV. Previous slab DFT studies found that the adsorption enthalpy with respect to gaseous ethene is slightly less exothermic on Pt{111}, with reported values of −1.26 eV[23] and −1.32 eV[24] for a H_2C-CH_2 species adsorbed at a bridge position in a di-σ fashion.

The next most energetically competitive ethene structure we found involves the hydrocarbon fragment bonding in a π-like fashion to the surface at a ridge atop site. The C−C bond is 1.40 Å long and is aligned along the $\langle 001 \rangle$ surface direction. The average H−C−C angle is 120.0°, and the shortest C−Pt bond length is 2.15 Å. Our assignment of a flat-lying π-bonded species is consistent with experimental results on Pt{111}, where at surface temperatures below 52 K a π-bonded H_2C-CH_2 species was observed by UPS[12] and RAIRS,[16] for which the C−C bond is also parallel to the surface.

The most stable di-σ ethene structure characterized in our study compares well to literature slab DFT results for H_2C-CH_2 adsorption on Pt{111}[23,24] and on Pd{111},[22] which found the C−C bonds in the di-σ form to be 1.48 Å and 1.44 Å, respectively, with a corresponding C−Pt bond length of 2.10 Å and a C−Pd bond length of 2.19 Å. Similar agreement is found between the π-bonded structures: The C−C bond length reported on Pt{111} is 1.41 Å with the C−Pt bond at 2.12 Å,[24] while on Pd{111}, the C−C bond length was found to be 1.38 Å, with the C−Pd bond 2.20 Å long.[22]

The most stable chemisorbed ethylidene, $HC-CH_3$ structure, labeled 1 in Figure 4, is found to be 0.23 eV less thermodynamically stable than ethene on Pt{110}(1 × 2). The unsaturated carbon atom bonds in a symmetrical bridge fashion to neighboring ridge Pt atoms, while the saturated CH_3 group points upward, with the C−C bond at an approximate 45° tilt to the surface normal. The C−C bond projects along the $\langle 001 \rangle$ surface direction and is 1.48 Å long. The two shortest C−Pt distances are 2.05 Å. This structure is also in good agreement with literature results for Pd{111}, which found the C−C bond distance for $HC-CH_3$ adsorbed at a bridge site to be 1.50 Å, with the shortest C−Pd length at 2.03 Å.[22]

On the basis of the large and exothermic computed enthalpy for adsorption, ethene is predicted to readily chemisorb on Pt{110}. This result is in agreement with a large number of previous experimental studies, which showed that ethene adsorbs reversibly on Pt at low temperatures and decomposes into various intermediates at room temperature or above. The nature of these intermediates depends on the crystallographic orientation of the surface and the temperature of adsorption.[10,11,13,17,35−47] Yagasaki et al.[11] have found at least two different species on

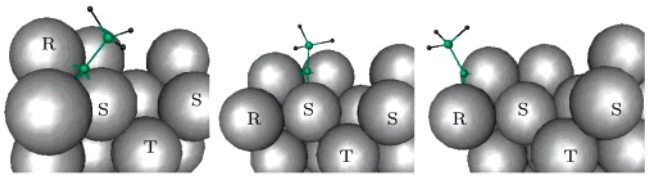

Figure 5. Ethylidyne chemisorbed local minima on Pt{110} numbered according to their relative energetic stabilities: 1 is the most stable, and 3 the least.

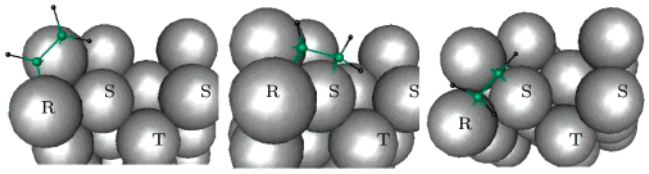

Figure 6. Vinyl chemisorbed local minima on Pt{110} numbered according to relative energetic stability: 1 is the most stable, and 3 the least.

Pt{110}(1 × 2) at temperatures above 100 K using electron energy loss spectroscopy (EELS) and thermal desorption spectroscopy (TDS). For temperatures around 270 K, they only found evidence for di-σ bonded ethene, while at 300 K, they detected the presence of both C_2H_2 and C_2H_3. Low exposures of ethene produce mostly C_2H_2 species, while at saturation, there seems to be about twice as much C_2H_3 on the surface as C_2H_2. Furthermore, Stuck et al.[10] have measured the calorimetric heat of interaction for ethene with a Pt{110}(1 × 2) single crystal at 300 K and found it to be surface-coverage dependent. Between 0 and 0.5 ML of apparent accumulated coverage, ethene was found to adsorb irreversibly on Pt{110}. At low coverages, the differential adsorption heat is around 2.59 eV, and this value was ascribed to the formation of C_2H_2 on the surface. It then drops in several steps to 1.24 eV at 1.5 ML of apparent coverage, perhaps due to the formation of π-bonded ethene on the surface.[10]

Adsorbed C−CH₃ and HC−CH₂. Six ethylidyne (C−CH_3) and fifteen vinyl (HC−CH_2) chemisorbed structures were characterized. The relative energies and geometries for the three structures lowest in energy are given in Table 1 and Figures 5 and 6.

Three competitive C_2H_3 species are found within a range of 0.13 eV. Of these, two are nearly isoenergetic C−CH_3 species, labeled 1 and 2 in Figure 5, which chemisorb at threefold hollow sites involving ridge and second-layer surface atoms. The fcc site is marginally preferred, by just 0.06 eV. This trend has also been previously observed by a slab DFT study of C−CH_3 adsorption on Pt{111},[23] for which the fcc site was found to be about 0.1 eV more stable than the hcp site, finding that is backed up by a low-energy electron diffraction (LEED) study.[38] For the fcc and hcp structures found in our study, the saturated CH_3 group is tilted somewhat toward the upright, with the corresponding C−C bond approximately at right angles to a ⟨111⟩ close-packed direction. Using eq 4, the enthalpy of dissociative adsorption for C−CH_3 structure **1** is exothermic by −1.16 eV, referenced with respect to C_2H_6 gas and the clean surface. For this structure, the shortest C−Pt bond length is 2.01 Å. The C−C bond length is 1.47 Å, similar in value to that for HC−CH_3 arranged at a bridge ridge site, suggesting an equivalent degree of hydrocarbon saturation for these structures. A C−C bond of 1.48 Å was previously reported for C−CH_3 adsorption at a fcc site by a theoretical study on Pt{111}, with the shortest C−Pt bond length of 1.16 Å.[23] Values of 1.49 Å for the C−C bond and 1.99 Å for the shortest C−Pd bond have been reported on Pd{111} over a threefold hollow site.[22]

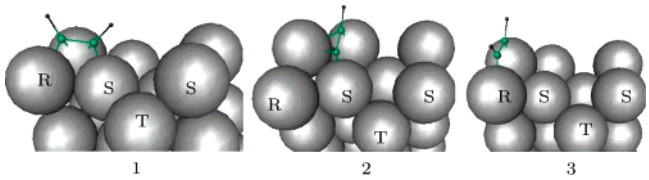

Figure 7. Ethyne local minima on Pt{110} numbered according to the relative energetic stability: Structure 1 is the most stable, and structure 3 the least.

A competitive chemisorbed vinyl species was found, labeled **1** in Figure 6. This structure bonds in an $\eta_1\eta_2$(C, C) fashion to the surface. The −CH group is bridging two neighboring ridge surface atoms at C−Pt distances of 2.15 Å and 2.01 Å, while the −CH_2 group is in a ridge atop site with a C−Pt distance of 2.18 Å. The C−C bond length is 1.40 Å. A theoretical study of vinyl chemisorption on Pd{111} found the −CH moiety over a bridge site with a C−Pd bond of 2.05 Å, while the −CH_2 group was bonded at an atop site with a C−Pd distance of 2.09 Å; the C−C bond was found to be 1.44 Å.[22] Interestingly, no competitive vinyl η_1(C) bonded structures are found on Pt{110}-(1 × 2), for which the −CH_2 fragment is not bonded to the surface. The vinyl structure labeled **10** in Supporting Information adopts such a bonding arrangement, but is 0.77 eV less stable than structure **1**.

Our theoretical study indicates that chemisorbed C−CH_3 and HC−CH_2 are almost equally stable on Pt{110}(1 × 2). Experimental studies on other metal surfaces have found a clear preference for only one of these species as the thermodynamic product. It is now widely accepted, for example, that ethene dehydrogenation over close-packed fcc {111} and hcp {0001} metal surfaces gives a stable C−CH_3 surface intermediate. On Pt{111}, ethene dehydrogenates to C−CH_3 in the temperature range 230−250 K.[13,17,35−47] For this surface, Zaera et al. have proposed that the dehydrogenation mechanism involves ethene isomerization to HC−CH_3, which then dehydrogenates to C−CH_3.[45] Above 400 K, C−CH_3 becomes unstable and decomposes to C−CH and CH.[45] Furthermore, thermodynamic cycles suggest that the metal−carbyne (Pt−C−CH_3) bond is very strong, around 3.11 eV, on Pt{111},[48] indicating a driving force for such bonds to be formed. Ethylidyne has also been identified spectroscopically on Pd{111}, Ir{111}, Rh{111}, and Ru{0001} as the product of ethylene adsorption.[49−52] Borg et al.[51] have, however, suggested a mechanistic pathway that involves ethene decomposition via a vinylic intermediate on Rh{111}. This then subsequently decomposes to ethylidyne.

In contrast, vinylic (vinyl and vinylidene) species were found experimentally to be the favored surface intermediates on more open surfaces such as Pt{110}(1 × 1), Ni{100}, and Pd-{100}.[49,50,53] Stable HC−CH_2 species were observed experimentally on Ni{110},[54,55] when ethene was adsorbed in the surface temperature range 160−200 K. Above 280 K, this intermediate decomposes to a mixture of C−CH and CH.

Our results suggest that Pt{110}(1 × 2) falls midway between the two C−CH_3 and H_2C−CH extremes. For this surface, it seems that the two species are of similar stability.

Adsorbed HC−CH and C−CH₂. Thirteen ethyne (HC−CH) and nine vinylidene (C−CH_2) adsorbed structures were characterized. The relative energies and geometries for the three structures lowest in energy are given in Table 1 and Figures 7 and 8.

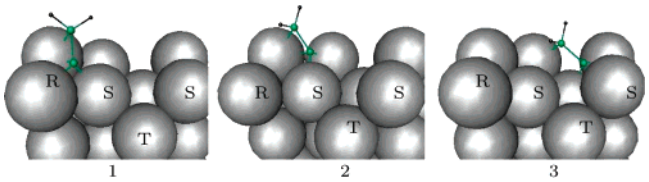

Figure 8. Vinylidene local minima on Pt{110} numbered according to the relative energetic stability: Structure 1 is the most stable, and 3 the least.

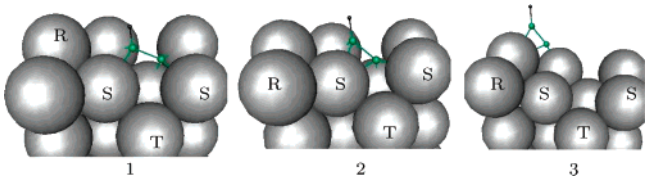

Figure 9. Ethynyl structures on Pt{110} numbered according to relative energetic stability: Structure 1 is the most stable, and 3 the least.

Ethyne and vinylidene are found to be energetically competitive. For the lowest-energy ethyne structure, labeled **1** in Figure 7, the enthalpy of dissociative adsorption with respect to gaseous ethane is −1.09 eV (using eq 4). One carbon atom bridges two neighboring ridge atoms 2.00 Å and 2.20 Å away, while the other carbon bridges neighboring ridge and second-layer atoms 2.19 Å and 2.04 Å away. The C−C bond distance is 1.37 Å, compared to a value of 1.20 Å for gas-phase ethyne.[56] Weakening of the C−C bond compared to the gas phase is believed to occur through mixing of the filled ethyne π orbital with an empty metal d orbital, while the empty π^* orbital overlaps a filled metal d orbital.[57] Each C−H bond has bent upward with respect to the C−C axis, with an average H−C−C angle of 127.1° suggesting, again, rehybridization of carbon atomic orbitals from sp toward sp^2. The next lowest chemisorbed HC−CH structure found by our study, labeled **2** in Figure 7, has each carbon atom bridging the same ridge site 2.18 Å away and neighboring second-layer surface sites 2.02 Å away. The C−C bond distance has also lengthened to 1.37 Å. Previous DFT studies on Pd{111} are in broad agreement with the current results and found HC−CH adsorption over a threefold fcc hollow site to give bridging C−Pd bond lengths of 2.20 Å and 2.01 Å, with a C−C bond of 1.36 Å.[22]

Vinylidene is unstable in the free state but is known to form stable complexes with transition metals.[58] In these complexes, vinylidene is a two-electron donor and may act as a terminal or bridging ligand. Our study finds that $C-CH_2$ is stabilized by adsorption onto Pt{110}(1 × 2). The lowest-energy structure of this type is approximately isoenergetic with that for chemisorbed ethyne. For the lowest minimum, labeled **1** in Figure 8, the enthalpy of dissociative adsorption with respect to gaseous ethane is −1.06 eV (using eq 4). The unsaturated −C fragment bonds at a threefold hollow site between two ridge atoms and one second layer atom, each 2.04 Å away on average. The $-CH_2$ fragment is over an atop ridge surface site, with a C−Pt bond of 2.22 Å. The C−H bonds are 1.08 Å and make an angle of 120° with the C−C bond, itself 1.38 Å long. Using ab initio methods, Dykstra et al.[59] have found a C−C bond length of 1.34 Å for gas-phase $C-CH_2$. The small C−C bond elongation over the surface compared to the gas phase suggests that backbonding is not as significant as for ethyne. On Pd{111}, a theoretical study found a structure for which the most unsaturated carbon atom is at a threefold hollow site, with an average C−Pd bond length of 1.97 Å, and the $-CH_2$ fragment over a neighboring atop site with a C−Pd distance of 2.31 Å.[22]

The current study finds that vinylidene structures **2** and **3** in Figure 8 are nearly isoenergetic, both around 0.25 eV less stable than $C-CH_2$ structure **1**. Structure **3** is unusual, as it involves the hydrocarbon bridging between two adjacent microfacets over the trough. The unsaturated −C fragment is positioned over a threefold hollow site, on average 2.04 Å away from each surface atom to which it bonds. The $-CH_2$ fragment binds in an atop fashion to a second-layer Pt atom on the other side of the trough, with a C−Pt distance of 2.14 Å. The C−C bond length has extended to a value of 1.44 Å, suggesting that the hydrocarbon adjusts its geometry for maximum bonding to the surface.

To recap, our study has found ethyne and vinylidene to be energetically competitive on Pt{110}(1 × 2) and to be stabilized over sites involving ridge atoms. Using supersonic molecular beams, Harris et al.[9] found the stable dissociation product of ethane on Pt{110}(1 × 2) at all coverages in the surface temperature range 350−400 K to have C_2H_2 stoichiometry. This species then decomposes to C_2H above 400 K, with a reaction-limited peak temperature of 430 K. Yagasaki et al.[11] have studied ethene thermal decomposition on Pt{110}(1 × 2) using HREELS and found a mixture of C_2H_2 and C_2H_3 at 300 K. The $-CH_2$ wag and scissor modes were observed at 990 cm^{-1} and 1420 cm^{-1}, respectively, which was interpreted as indicating that the C_2H_2 surface species observed is in fact vinylidene, with no ethyne being formed. The proportion of $C-CH_2$ compared to $C-CH_3$ is higher at lower coverages, as expected for an adlayer containing a mixture of species. Stuck et al.,[10] in a study of ethene adsorption on Pt{110}(1 × 2) at 300 K, found that C_2H_2 is formed at very low surface coverages, while at higher coverages, the surface products were the more fully hydrogenated $C-CH_3$ and H_2C-CH_2 species. Product mixtures below 300 K were interpreted in terms of the presence of coadsorbed hydrogen on the surface at these temperatures,[9] which was previously shown to inhibit the decomposition of $HC-CH_3$ and H_2C-CH_2 on Pt{111}.[17] At 370 K and above, adsorbed hydrogen might desorb as soon as it is formed on the surface, giving a pure C_2H_2 adlayer at all surface coverages as the product of ethane dissociative adsorption.[9] In contrast, no clear thermodynamic candidate emerges from our theoretical study when comparing the enthalpies of the most stable C_2H_x ($x = 0-5$) chemisorbed species with gaseous ethane and clean surface (using the reaction scheme given by eq 4). Further analysis of our data, taking gas-phase thermodynamics into account, is given below. Kinetic effects might also play a major role; this issue will be discussed in a forthcoming paper.

Experimental studies on Pd{111}[60] found that ethyne adsorbed at a surface temperature of 120 K is converted to vinylidene at 213 K, with further conversion to ethylidyne above 230 K. On Pt{111}, two adsorbed forms of ethyne were observed spectroscopically at 100 K.[61] A weakly distorted and a highly distorted, flat-lying species have been found, with C−C bond distances of 1.34−1.39 Å and 2.50 Å, in agreement with results from an earlier low-energy electron diffraction (LEED) study.[62] The C−C hybridization in the highly distorted species is around $sp^{2.5}$, with the C−C−H bond angle derived from spectroscopic measurements between 122° and 132° and in good agreement with the value of 120° deduced from vibrational electron energy loss spectroscopy (EELS) results.[63]

Adsorbed C−CH and C−C. Fifteen distinct ethynyl (C−CH) local minima were characterized. The relative energies and geometries for the three structures lowest in energy are given in Table 1 and Figure 9.

A clear thermodynamic preference of at least 0.49 eV for an $\eta_2\eta_3$ (C, C) structure, labeled **1** in Figure 9, was observed. For this structure, the enthalpy of dissociative adsorption with respect

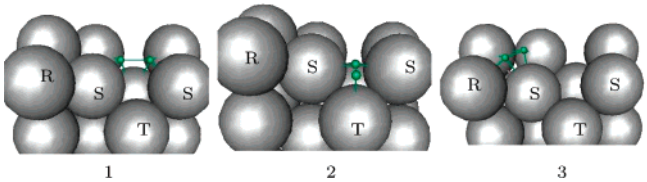

Figure 10. Carbidic ethynylene local minima on Pt{110} numbered according to relative stability: Structure 1 is the most stable, and 3 is the least.

to gaseous ethane is −1.05 eV (using eq 4). The most unsaturated carbon atom binds at a threefold hollow site involving two second-layer and one trough surface atoms, with an average C−Pt distance of 2.03 Å. The −CH fragment bridges two microfacet surface atoms across the trough, with an average C−Pt bond length of 2.10 Å. The C−C bond length is 1.41 Å, which is 0.04 Å longer than the value found for the more saturated, chemisorbed HC−CH structure **1** shown in Figure 7, suggesting that the hydrocarbon fragment readily adjusts its internal geometry to achieve maximum bonding to the surface. A theoretical study on Pd{111} found a structure where the most unsaturated C atom lies over a threefold Pd site with an average C−Pd distance of 1.99 Å, while the −CH fragment also bridges two Pd sites, on average 2.13 Å away.[22]

A comparison of the energetics for the various C−CH structures (Table 1) reveals that it is highly unfavorable for C−CH to adsorb over ridge and second-layer surface sites. This observation is in marked contrast with our results for chemisorption of more saturated C_2H_x species on the Pt{110}(1 × 2) surface, for which a strong stabilization at ridge surface sites is observed.

Temperature-programmed reaction (TPR) studies found that C_2H_2 decomposes to C_2H above 400 K, with a reaction-limited peak temperature of 430 K.[9] The high surface temperatures involved suggest either a high activation barrier for C_2H_2 dehydrogenation or that a thermodynamically less stable species is being formed on the surface. The kinetics for this process will be discussed in a future paper; however, comparing the stabilities of C_2H_2 and C−CH referenced relative to ethane gas and clean surface (using eq 4) does indeed confirm that C−CH is 0.04 eV less stable.

The ten carbidic ethynylene (C−C) geometries were characterized. The relative energies and geometries for the three structures lowest in energy are given in Table 1 and Figure 10.

A clear preference was found for an $\eta_3\eta_3$(C, C) carbidic structure centered over a trough atop site, labeled **1** in Figure 10. The C−C bond is 1.38 Å long and is aligned along the ⟨001⟩ direction. Each carbon atom bonds to the surface at a threefold site involving two second-layer and one trough atom, on average 2.10 Å away. For this structure, the enthalpy of dissociative adsorption with respect to gaseous ethane and the clean surface (eq 4) is −0.61 eV, which is 0.44 eV less stable than that for C−CH formation computed via the same reaction scheme. This result indicates that it is thermodynamically unfavorable to dissociate C−CH to C−C on Pt{110}(1 × 2) at low temperature, in agreement with experimental results by Harris et al.,[9] which found that C−CH dehydrogenates to give carbidic carbon only at rather high surface temperatures, above 600 K.

In fact, the energetics for complete ethane dehydrogenation on Pt{110}(1 × 2) may fruitfully be compared using two different reaction schemes. One scheme follows from eq 4 and yields as overall reaction products adsorbed C−C and six H adatoms. The other possibility is a modified scheme where the products for ethane dissociation are two carbon and six hydrogen adatoms

$$8Pt_{110}^{(2\times2)} + C_2H_6^{gas} \rightarrow 2C^{ads} + 6H^{ads} \quad (5)$$

In both schemes, the six H^{ads} and one C−C or two C^{ads} products are adsorbed on separate $Pt_{110}^{(2\times2)}$ slabs, and each dissociation product is arranged in its most stable geometry at a coverage of 0.25 ML. The theoretical data input into the two schemes for hydrogen and carbon adatom adsorption are from Petersen et al.[26,27] In the above model, the geometry for H-atom adsorption is, as before, over a ridge bridge site, while the C adatom is adsorbed over a fourfold site, involving second- and trough-layer atoms.

Ethane dehydrogenation to C adatoms is found to be exothermic by −0.70 eV, which is favorable by 0.09 eV compared to adsorbed C−C. The barrier for C−C bond scission is, however, likely to be considerably higher than for any of the C−H bonds. As previously discussed, the product for ethane dehydrogenation on Pt{100} was found experimentally to be a carbidic species at surface temperatures above 600 K.[9] However, the dissociation product was found to change if the experiments were carried out at 800 K where carbonaceous multilayers or graphite were found to form instead.[9] In view of our theoretical findings, these products could be carbon adatoms. If this is indeed the case, a buildup in the number of adsorbed C atoms on the surface to coverages of around 0.5 ML is expected to change the (1 × 2) surface reconstruction back to the (1 × 1) phase, as suggested by DFT results from Petersen et al.[26,27] and experimental results from Watson et al.[64]

Thermodynamic Analysis and Discussion

Surface energetics were investigated by comparing the free energy per supercell for the various chemisorbed C_2H_x species on the Pt{110}(1 × 2) surface.

For any given adsorbed C_2H_x species on $Pt_{110}^{(2\times2)}$, the free energy $F_{C_2H_x}$ is defined in terms of the internal energy per supercell, $E_{C_2H_x}$ (that is, the DFT adsorption energy at absolute zero) and the chemical potentials of the constituent atomic species, μ_C and μ_H

$$F_{C_2H_x} = E_{C_2H_x} - 2\mu_C - x\mu_H \quad (6)$$

Within this description, the variation in the number of atoms present for different adsorbed hydrocarbon fragments is automatically canceled by the terms in the summation. As a result, the preference for the system to adopt a particular structure over the others is evaluated simply by comparing their free energies, provided that the chemical potentials of the constituent species are available. The C_2H_x on $Pt_{110}^{(2\times2)}$ chemisorbed structure with the lowest free energy at temperature T and total pressure P is hence thermodynamically preferred under these external constraints. Furthermore, all the chemisorbed C_2H_x structures investigated are based on a common (2 × 2) supercell. This simplifies our description further, since we do not need to explicitly consider the chemical potential of the metal surface. However, we note that this value would have been readily available if needed, since the surface is in thermal equilibrium with its bulk, implying that the surface chemical potential must necessarily equal the bulk chemical potential (which is in turn given by the total energy per atom in the bulk structure). The chemical potentials for the constituent carbon and hydrogen atoms at temperature T and total pressure P are obtained if each adsorbed C_2H_x species on $Pt_{110}^{(2\times2)}$ is held in thermal equilibrium

with the other adsorbed surface species and with a gas of carbon- and hydrogen-containing molecules. In the present case, we anticipate the dominant gas-phase species to be ethane, ethene, ethyne, and hydrogen. The chemical potentials for the carbon and hydrogen atoms, μ_i, are then obtained from

$$\mu_{H_2}(T, p) = 2\mu_H \tag{7}$$

$$\mu_{C_2H_x}(T, p) = 2\mu_C + x\mu_H \tag{8}$$

Note that p in each case is to be interpreted as the partial pressure of the species on the left-hand side and that the system of equations must be simultaneously satisfied, implying that only two of these partial pressures may be independently chosen.

The chemical potentials for a gas of molecules X can be computed from experimental data by reference to the gas-phase thermodynamics. If we deal with each gas-phase species separately, its (T, p) dependent chemical potential μ_X becomes

$$\mu_X(T, p) = \left.\frac{\partial G_X}{\partial N_X}\right|_{T,p} \tag{9}$$

where G_X and N_X are the respective Gibbs free energy and number of molecules involved.

Infinitesimal changes in the Gibbs free energy at temperature T can be expressed in terms of corresponding changes in the enthalpy, H_X, and entropy, S_X, according to

$$dG_X = dH_X - T\,dS_X \tag{10}$$

As a result, the chemical potential for gas-phase species X is given by

$$\mu_X(T, p) = \left.\frac{\partial H_X}{\partial N_X}\right|_{T,p} - T\left.\frac{\partial S_X}{\partial N_X}\right|_{T,p} \tag{11}$$

Assuming that ideal gas behavior holds, the (T, $p^\ominus$) dependent chemical potentials can be expressed in terms of the molar enthalpy H_X and molar entropy S_X

$$\mu_X(T, p^\ominus) = \frac{1}{N_A}[H_X(T, p^\Theta) - TS_X(T, p^\ominus)] \tag{12}$$

where $p^\ominus$ denotes standard pressure and is equal to 1.013×10^6 mbar, and N_A is Avogadro's number.

Experimental values for the molar entropies of gaseous hydrogen, $S_{H_2}(T, p^\ominus)$, are available at a range of temperatures T and standard pressure.[31] The molar enthalpies of hydrogen are also available at standard pressure and a range of temperatures, and are tabulated in the form of the corresponding difference from the value at standard temperature $T^\ominus = 298.15$ K and standard pressure $p^\ominus$, i.e., in the form $\Delta H_{H_2}(T^\ominus, p^\ominus \rightarrow T, p^\ominus)$.[31] Since the increase in molar enthalpy on going from absolute zero temperature and pressure up to standard temperature and pressure is also known, $\Delta H_{H_2}(0, 0 \rightarrow T^\ominus, p^\ominus) = 8.468$ kJ mol^{-1}, the molar enthalpy for gaseous hydrogen at some temperature T and standard pressure becomes

$$H_{H_2}(T, p^\ominus) = H_{H_2}(T^\ominus, p^\ominus) + \Delta H_{H_2}(T^\ominus, p^\ominus \rightarrow T, p^\ominus) \tag{13}$$

$$H_{H_2}(T^\ominus, p^\ominus) = H_{H_2}(0, 0) + \Delta H_{H_2}(0, 0 \rightarrow T^\ominus, p^\ominus) \tag{14}$$

In this scheme, the value of $H_{H_2}(0, 0)$ is computed using DFT, employing convergence parameters comparable to those used in computing the structures of C_2H_x species adsorbed on $Pt_{110}^{(2\times2)}$. We find $H_{H_2}(0, 0) = -3065.370$ kJ mol^{-1}. The resulting thermodynamic parameters for molecular hydrogen are summarized in the Supporting Information. Experimental values for the molar entropies of gaseous ethane, ethene, and ethyne, $S_X(T, p^\ominus)$, are also available at a range of temperatures at standard pressure. In computing their corresponding molar enthalpies, $H_X(T, p^\ominus)$, however, there is a further complication compared to the gaseous hydrogen case, because $\Delta H_X(0, 0 \rightarrow T^\ominus, p^\ominus)$ is not available. Nevertheless, using the enthalpy of formation for these gaseous species at standard temperature and pressure, $\Delta H_{fX}(T^\ominus, p^\ominus)$, for which values are given in the Supporting Information, gets around this problem. But now, for

$$H_X(T, p^\ominus) = H_X(T^\ominus, p^\ominus) + \Delta H_X(T^\ominus, p^\ominus \rightarrow T, p^\ominus) \tag{15}$$

ethene, for example

$$H_X(T^\ominus, p^\ominus) = 2H_C(T^\ominus, p^\ominus) + 2H_{H_2}(T^\ominus, p^\ominus) + \Delta H_{fX}(T^\ominus, p^\ominus) \tag{16}$$

where $H_C(T^\ominus, p^\ominus)$ is the molar enthalpy of graphitic carbon at standard temperature and pressure. The change in enthalpy for graphite between absolute zero temperature and standard temperature, $\Delta H_C(0, 0 \rightarrow T^\ominus, p^\ominus)$, is 1.050 kJ mol^{-1}.[31] Since the enthalpy of a solid is independent of pressure in the experimentally accessible regimes, we obtain

$$H_C(T^\ominus, p^\ominus) = H_C(0, 0) + \Delta H_C(0, 0 \rightarrow T^\ominus, p^\ominus) \tag{17}$$

We find $H_C(0, 0)$ to be -156.197 eV per C atom (equivalent to $-15\,070.719$ kJ mol^{-1}) as computed by DFT. Hence, $H_C(T^\ominus, p^\ominus)$ is $-15\,069.669$ kJ mol^{-1}. The molar enthalpies at temperature T and standard pressure, $H_X(T, p^\ominus)$, together with the chemical potentials $\mu_X(T, p^\ominus)$ for gaseous ethane, ethene, and ethyne, are tabulated in the Supporting Information.

The chemical potentials for gaseous hydrogen, ethane, ethene, and ethyne at any temperature T and pressure p, $\mu_X(T, p)$, are related to their chemical potentials at temperature T and standard pressure $p^\ominus$, $\mu_X(T, p^\ominus)$, according to

$$\mu_X(T, p) = \mu_X(T, p^\ominus) + kT\ln\left(\frac{p}{p^\ominus}\right) \tag{18}$$

The chemical potentials for the gaseous species were computed via the above scheme at a range of temperatures and pressures (see Tables in Supporting Information; part III). Since the chemical potentials for these molecular species can also be written as the sum of the chemical potentials for their constituent atoms according to eqs 7 and 8, we were hence able to compute the free energies for each of the C_2H_x ($x = 0-5$) species adsorbed on $Pt_{110}^{(2\times2)}$ using eq 6. The raw DFT internal energies per (2 × 2) cell (i.e., per molecule) are listed in a table in the Supporting Information (part III) for the most stable geometry of each species.

To provide a simple example of the kind of information that may be extracted through this analysis, we have chosen to specify the partial pressures of gaseous hydrogen and ethene in the following discussion, leaving the partial pressures of ethane and ethyne as implicit variables. In principle, of course, we could have chosen to specify the partial pressures of *any* two of the gas-phase species (or indeed the partial pressure of just one, together with the total pressure).

We begin by investigating a low-pressure regime, broadly corresponding to the circumstances of a typical ultrahigh vacuum (UHV) experiment. To do this, we set $p_{H_2} = p_{C_2H_4} = 10^{-10}$

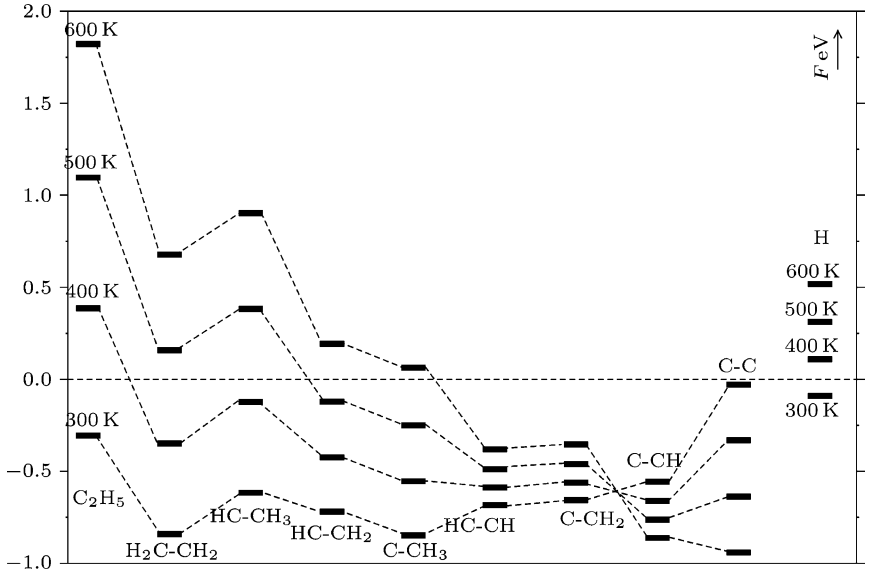

Figure 11. Free energy, F, of adsorbed C_2H_x species on Pt{110}(1 × 2) in eV. The partial pressures of hydrogen and ethene are $p/p^{\ominus} = 1 \times 10^{-13}$. The clean surface is taken as the energy zero.

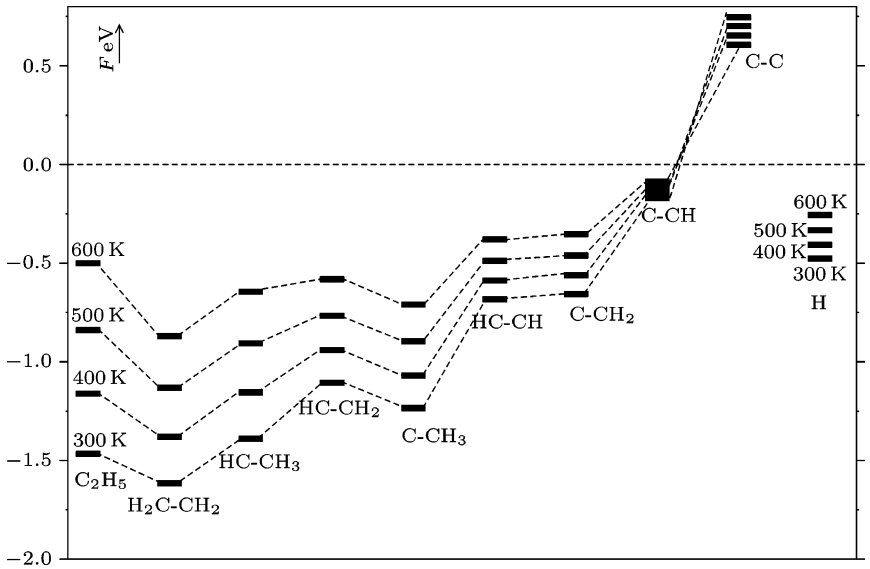

Figure 12. Free energy, F, of adsorbed C_2H_x species on Pt{110}(1 × 2) in eV. The partial pressures of hydrogen and ethene are $p/p^{\ominus} = 1 \times 10^{0}$. The clean surface is taken as the energy zero.

mbar (i.e., $10^{-13}/p^{\ominus}$) and consider temperatures in the range 300−600 K. The resulting free energies are depicted in Figure 11. We note that only the lowest-energy geometry has been used for each species in constructing this graph, even though it is conceivable that vibrational entropy in the adsorbed molecule might induce site-switching at elevated temperatures. We do not, however, believe that this is particularly likely, given that the energy separations between the lowest and second-lowest energy geometries of the same species are typically relatively large (the exceptions being ethylidyne and ethene). Omission of vibrationally induced site-switching is therefore unlikely to lead to significant error. Furthermore, we note that the separation in free energy between different hydrocarbon species is also generally fairly large, so that any small adjustments due to neglected vibrational effects will not substantially change our conclusions.

It is immediately clear that species containing significant numbers of hydrogen atoms (i.e., C_2H_5 to C_2H_2) are strongly destabilized as the temperature is raised because of the increasing entropic preference for hydrogen to enter the gas phase, while the more dehydrogenated products (i.e., C_2H and C_2) are actually stabilized, because the entropic driving force for hydrocarbons to enter the gas phase rises more slowly. The equilibrium H_2 desorption temperature estimated from the free energy model is approximately 350 K in this pressure range, agreeing very well with the nonequilibrium desorption peak at about 370 K observed in temperature-programmed desorption experiments.[9] The hydrocarbon thermal behavior is more complex but may be summarized as follows: At 300 K, the preferred surface species are ethene (H_2C-CH_2) and ethylidyne ($C-CH_3$), consistent with the results of ethene adsorption at 300 K reported by Stuck et al.[10] As the temperature is raised, ethene is substantially destabilized, and somewhere in the region of 350 K, four different surface species become competitive: ethylidyne ($C-CH_3$), ethyne ($HC-CH$), vinylidene ($C-CH_2$), and ethynyl ($C-CH$). Should all four species occur in equal concentrations, the resulting average C_2H_2 stoichiometry would be consistent with that found experimentally by Harris et al.[9] as the result of ethane dissociation at 350−400 K. It should be noted, however, that those results were interpreted as indicating

a single C_2H_2 species, rather than a mixture; our results are not inconsistent with such a conclusion but would imply that suppression of C−CH_3, C−CH, and *either* HC−CH or C−CH_2 is due to kinetic effects beyond the scope of the present paper. By around 400 K, our free energy diagram begins to show a clear preference for ethynyl (C−CH) as the stable surface species, again consistent with the work of Harris et al.[9] which showed decomposition of adsorbed C_2H_2 to C_2H at 430 K. Finally, we note that adsorbed ethynylene (C−C) becomes the dominant product in our calculations at around 600 K, once more matching well with the reported experimental behavior.[9]

At this stage, we should introduce the important caveat that it is highly dubious whether molecular beam and temperature-programmed reaction/desorption experiments correspond even approximately to equilibrium conditions; not only are there obvious time factors involved in achieving surface equilibrium, but it is also not clear to what extent the residual gas in a UHV chamber can be thought of as being in thermal equilibrium with a hot crystal when it is clearly also in thermal contact with the much larger heat sink of the chamber walls. This raises the question of what temperature to ascribe to the gas-phase molecules—the surface temperature or the wall temperature? Clearly, our discussion above has assumed that it is reasonable to treat the gas phase as being held at the same temperature as the surface, and the close similarity between the present theoretical results and experimental observation[9−11] strongly suggests that this is not a bad approximation. We justify this approach by appealing to a two-fluid model in which one fluid consists of molecules that have reached near-equilibrium with the chamber walls, while the other consists of recently desorbed molecules that have yet to suffer any subsequent collisions and thus display an energy distribution consistent with the surface temperature. In those UHV experiments where net desorption takes place or where a constant surface coverage is maintained by means of a molecular beam, the number of molecules traveling outward through the near-surface region will far exceed the number entering it from the residual gas, so the region close to the surface can be thought of as dominated by the fluid component having a temperature similar to that of the surface. In other words, the fact that these experiments are dominated by desorption rather than adsorption means that we can treat the surface as being in a state of quasi-equilibrium with the desorbing component of the gas, neglecting the fact that the adsorbing component will be at a different temperature.

In contrast to the low-pressure regime, substituting $p_{H_2} = p_{C_2H_4} = 10^0$ bar leads to far less complex thermal chemistry, with smaller temperature-induced shifts in the free energies and less variation as a function of stoichiometry (Figure 12). The most stable species is found to be ethene (H_2C-CH_2) throughout the entire 300−600 K temperature range, albeit with ethylidyne (C−CH_3) becoming relatively competitive toward the higher end. Such significant differences from the UHV case underline the importance of thermodynamic arguments in bridging the pressure gap between surface science experiments and more realistic catalytic conditions.

Conclusion

The DFT results reported in this work allow us to construct a rather complete picture of C_2H_x species on Pt{110}(1 × 2). We find that the preferred geometry in each case is one that completes the tetravalency of the carbon atoms while maximizing the number of platinum atoms involved. In general, the more hydrogenated compounds tend to bind most strongly in the vicinity of the ridge, with the trough preferred only by C−CH and C−C species. Such trends are strongly reminiscent of previous calculations for CH_x species at the same surface[26,27,29] and point toward possible regularities that might be borne out in future work on higher alkanes.

Analysis of the thermodynamic stability of C_2H_x surface species through a free energy approach provides future insight, concurring with prior UHV experimental findings that ethene and ethylidyne are favored at low temperatures, with ethynyl and eventually ethynylene becoming dominant at around 400 and 600 K, respectively. Crucially, such analysis allows one to bridge the pressure gap between UHV work and real catalysis, simply by varying the appropriate gas-phase parameters.

Acknowledgment. We acknowledge support from The Royal Society (S.J.J.) and a studentship from the EPSRC (A.T.A.).

Supporting Information Available: The atomic coordinates and raw DFT internal energies per (2 × 2) unit cell for all characterized structures, together with data used to compute the free energies for the most stable species. This material is available free of charge via the Internet at http://pubs.acs.org.

References and Notes

(1) Bodke, A. S.; Olschki, D. A.; Schmidt, L. D.; Ranzi, E. *Science* **1999**, *285*, 712.
(2) Somorjai, G. A. *Introduction to Surface Chemistry and Catalysis*; Wiley: New York, 1994.
(3) Horiuti, I.; Polanyi, M. *Trans. Faraday Soc.* **1934**, *30*, 1164.
(4) Rostrup-Nielsen, J. R. *Catal. Today* **2000**, *63*, 159.
(5) Dry, M. *Catal. Today* **2002**, *71*, 227.
(6) Davis, S. M.; Somorjai, G. A. *Hydrocarbon conversion over metal surfaces*; King, D. A., Woodruff, D. P., Eds.; Elsevier Scientific: Amsterdam, 1982.
(7) Low, J. J.; Goddard, W. A., III *Organometallics* **1986**, *5*, 609.
(8) Kua, J.; Goddard, W. A., III *J. Phys. Chem. B* **1998**, *102*, 9492.
(9) Harris, J. J. W.; Fiorin, V.; Campbell, C. T.; King, D. A. *J. Phys. Chem. B* **2005**, *109*, 4069.
(10) Stuck, A.; Wartnaby, C. E.; Yeo, Y. Y.; King, D. A. *Phys. Rev. Lett.* **1995**, *74*, 578.
(11) Yagasaki, E.; Backman, A. L.; Masel, R. I. *J. Phys. Chem.* **1990**, *94*, 1066.
(12) Cassuto, A.; Kiss, J.; White, J. M. *Surf. Sci.* **1991**, *255*, 289.
(13) Cremer, P. S.; Su, X.; Shen, Y. R.; Somorjai, G. A. *J. Am. Chem. Soc.* **1996**, *118*, 2942.
(14) Fan, J.; Trenary, M. *Langmuir* **1994**, *9* (10), 364.
(15) Kubota, J.; Ichihara, S.; Kondo, J. N.; Domen, K.; Hirose, C. *Langmuir* **1996**, *12*, 1926.
(16) Kubota, J.; Ichihara, S.; Kondo, J. N.; Domen, K.; Hirose, C. *Surf. Sci.* **1996**, *357*, 634.
(17) Land, T. A.; Michely, T.; Behm, R. J.; Hemminger, J. C.; Comsa, G. *J. Chem. Phys.* **1992**, *97*, 6774.
(18) Zaera, F. *Langmuir* **1996**, *12*, 88.
(19) Wang, L. P.; Tysoe, W. T.; Hoffman, H.; Zaera, F.; Ormerod, R. M.; Lambert, R. M. *Surf. Sci.***1990**, *94*, 4236.
(20) Neurock, M.; Van Santen, R. A. *J. Phys. Chem. B* **2000**, *104*, 1127.
(21) Stacchiola, D.; Burkholder, L.; Tysoe, W. T. *Surf. Sci.* **2002**, *511*, 215.
(22) Pallassana, V.; Neurock, M.; Lusvardi, V. S.; Lerou, J. J.; Kragten, D. D.; van Santen, R. A. *J. Phys. Chem. B* **2002**, *106*, 1656.
(23) Ge, Q.; King, D. A. *J. Chem. Phys.* **1999**, *110*, 4699.
(24) Watson, G. W.; Wells, R. P. K.; Willock, D. J.; Hutchings, G. J. *J. Phys. Chem. B* **2000**, *104*, 6439.
(25) Papoian, G.; Nørskov, J. K.; Hoffmann, R. *J. Am. Chem. Soc.* **2000**, *122*, 4129.
(26) Petersen, M. A.; Jenkins, S. J.; King, D. A. *J. Phys. Chem. B* **2004**, *108*, 5909.
(27) Petersen, M. A.; Jenkins, S. J.; King, D. A. *J. Phys. Chem. B* **2004**, *108*, 5920.
(28) Payne, M. C.; Teter, M. P.; Allan, D. C.; Arias, T. A.; Joannopoulos, J. D. *Rev. Mod. Phys.* **1992**, *64*, 1045.
(29) Anghel, A. T.; Wales, D. J.; Jenkins, S. J.; King, D. A. *Phys. Rev. B* **2005**, *71*, 113410.
(30) Anghel, A. T.; Wales, D. J.; Jenkins, S. J.; King, D. A. *Chem. Phys. Lett.* **2005**, *413*, 289.

(31) *CRC Handbook of Chemistry and Physics*, 79th ed.; Lide, D. R., Ed.; CRC Press: Boca Raton, 1998.
(32) Steininger, H.; Ibach, H.; Lehwald, S. *Surf. Sci.* **1982**, *17*, 685.
(33) Felter, T. E.; Weinberg, W. H. *Surf. Sci.* **1981**, *103*, 265.
(34) Stohr, J.; Sette, F.; Johnston, A. L. *Phys. Rev. Lett.* **1984**, *53*, 1684.
(35) Carter, E. A.; Koel, B. E. *Surf. Sci.* **1990**, *226*, 339.
(36) Erley, W.; Li, Y.; Land, D. P.; Hemminger, J. C. *Surf. Sci.* **1994**, *301*, 177.
(37) Yeo, Y. Y.; Stuck, A.; Wartnaby, C. E.; King, D. A. *Chem. Phys. Lett.* **1996**, *259*, 28.
(38) Starke, U.; Barbieri, A.; Materer, N.; van Hove, M. A.; Somorjai, G. A. *Surf. Sci.* **1992**, *286*, 1.
(39) Zaera, F.; Janssens, T. V. W.; Ofner, H. *Surf. Sci.* **1996**, *368*, 371.
(40) Cremer, P. S.; Stanners, C.; Niemantsverdriet, J. W.; Shen, Y. R.; Somorjai, G. A. *Surf. Sci.* **1995**, *328*, 111.
(41) Ohtani, T.; Kubota, J.; Kondo, J. N.; Hirose, C.; Domen, K. *Surf. Sci.* **1998**, *415*, 983.
(42) Ofner, H.; Zaera, F. *J. Phys. Chem. B* **1997**, *101*, 396.
(43) Zaera, F. *J. Phys. Chem.* **1990**, *94*, 8350.
(44) Zaera, F. *J. Phys. Chem.* **1990**, *94*, 5090.
(45) Zaera, F.; French, C. R. *J. Am. Chem. Soc.* **1999**, *121*, 2236.
(46) Steininger, H.; Ibach, H.; Lehwald, S. *Surf. Sci.* **1982**, *117*, 685.
(47) Yata, M.; Madix, R. J. *Surf. Sci.* **1995**, *328*, 171.
(48) Kesmodel, L. L.; Dubois, L. H.; Somorjai, G. A. *J. Chem. Phys.* **1979**, *70*, 2180.
(49) Masel, R. I. *Principles of Adsorption and Reaction on Solid Surfaces*; Wiley: New York, 1996.
(50) Yagasaki, E.; Masel, R. I. *Catalysis* **1994**, *11*, 165.
(51) Borg, H. J.; van Hardeveld, R. M.; Niemantsverdriet, J. W. *J. Chem. Soc., Faraday Trans.* **1995**, *91*, 3679.
(52) Parlett, P. M.; Chesters, M. A. *Surf. Sci.* **1996**, *357*, 791.
(53) Stuve, E. M.; Madix, R. J. *J. Phys. Chem.* **1985**, *89*, 105.
(54) Hutson, F. L.; Ramaker, D. E.; Koel, B. E.; Gebhard, S. C. *Surf. Sci.* **1991**, *248*, 119.
(55) Zhu, X.-Y.; Castro, M. E.; Akhter, S.; White, J. M.; Houston, J. E. *Surf. Sci.* **1988**, *207*, 1.
(56) Herzberg, G. *Molecular spectra and molecular structure*; Van Nostrand-Reinhold: Princeton, NJ, 1966; Vol. III.
(57) Chatt, J.; Duncanson, L. A. *J. Chem. Soc.* **1953**, 2939.
(58) Antonova, A. B.; Kolobova, N. E.; Petrovsky, P. V.; Lokshin, B. V.; Obezyuk, N. S. *J. Organomet. Chem.* **1977**, *137*, 55.
(59) Dykstra, C. E.; Schaefer, H. F., III *J. Am. Chem. Soc.* **1978**, *100*, 1378.
(60) Jungwirthova, I.; Kesmodel, L. L. *J. Phys. Chem. B* **2001**, *105*, 674.
(61) Demuth, J. E. *Surf. Sci.* **1979**, *84*, 315.
(62) Kesmodel, L. L.; Baetzold, R.; Somorjai, G. A. *Surf. Sci.* **1977**, *66*, 299.
(63) Ibach, H.; Lehwald, S. *J. Vac. Sci. Technol.* **1978**, *15*, 407.
(64) Watson, D. T. P.; Titmuss, S.; King, D. A. *Surf. Sci.* **2002**, *505*, 49.